

Optimized Mechanical And Impact Performance Of High Strength Tempo Oxidized Cellulose Nanofibril (TOCNF) - Epoxy Laminates

Endrina Stefani Forti

Purdue University

Daniela Betancourt-Jimenez

Purdue University

Gregory T Schueneman

USDA Forest Products Laboratory

Robert J Moon

USDA Forest Products Laboratory

Jeffrey Youngblood (✉ jpyoungb@purdue.edu)

Purdue University <https://orcid.org/0000-0002-8720-8642>

Research Article

Keywords: TEMPO cellulose nanofibril (TOCNF) laminates, epoxy laminates

Posted Date: May 11th, 2021

DOI: <https://doi.org/10.21203/rs.3.rs-461256/v1>

License:   This work is licensed under a Creative Commons Attribution 4.0 International License.

[Read Full License](#)

Abstract

In this work, TEMPO cellulose nanofibril (TOCNF) laminates were fabricated using a layup method. Two different TOCNF layers were tested, a neat TOCNF and a TOCNF with polyvinyl alcohol (PVA) strengthening aid with four different epoxy formulations as interlayers for the laminates. Flexural testing showed a correlation between the presence of stronger layers (TOCNF + PVA) in the laminate with a higher flexural strength, bending modulus, and work of failure. Different modes of fracture within the laminates occurred based on epoxy type. A stiffer epoxy generated a reduced mechanical response and substantial interlayer damage. On the other hand, a more ductile epoxy increased the WOF of the laminates, inducing a higher delamination at the interface. The addition of a silane coupling agent (APTES) resulted in a higher compatibility between the TOCNF and epoxy, generating an increased ultimate tensile strength (UTS) and a decreased energy to rupture associated with the reduction of crack digression mechanisms in the system. In general, laminates with stronger TOCNF layers (TOCNF + PVA) and increased adhesion (APTES), showed a flexural strength increase of 61%, a bending modulus increase of 80% and the same WOF when compared with the original laminates. Finally, impact testing of TOCNF materials was performed for the first time in literature, the specific energy to rupture of laminates was comparable to those achieved by acrylic and borosilicate glass, while maintaining a higher or similar specific strength to glass. Laminates showed good transparency and low haziness.

Introduction

TEMPO (2,2,6,6-tetramethylpiperidine-1-oxyl)-oxidized cellulose nanofibrils (TOCNF) are polysaccharide nanomaterials that are extracted mainly from wood, plants and other biomass sources (Isogai et al. 2011; Moon et al. 2011; Clarkson et al. 2020). These materials have attracted attention due to their sustainable and bio-renewable nature and are usually produced by chemically aided methods, where the catalyst TEMPO is used in conjunction with a primary oxidizer (usually hypochlorite or chlorite) to convert the primary hydroxyl groups on the surface of the fibrils to carboxylic acids. The reaction, which is usually carry out in water, helps loosen the bonds between cellulose such that mechanical action can produce a suspension of negatively charged fibrils that are several microns long and around 2–3 nm wide. Neat TOCNF suspensions and high percentage TOCNF mixtures can be cast to produce totally transparent films with exceptional mechanical properties, with Young's modulus up to 20 GPa and ultimate tensile strength (UTS) of around 300 MPa (Saito et al. 2009; Isogai et al. 2011; Moon et al. 2011; Fujisawa et al. 2011; Benítez and Walther 2017; Forti et al. 2020; Clarkson et al. 2020; Endrina S. Forti, Sami M. El Awad Azrak, Xin Y. Ng, Whirang Cho, Gregory T. Schueneman, Robert J. Moon, Douglas M. Fox 2021). Even when films show high strength and stiffness, their brittleness and the high residual stresses generated within the films during drying, makes the production of thick materials difficult and reduce the potential for industrial applications (Forti et al. 2020).

In a previous publication, a potential solution to TOCNF scalability problems was introduced. Layup structures of TOCNF were prepared with improved mechanical properties both in bending and tension, creating thicker TOCNF materials while decreasing the inherent brittleness of TOCNF. The effect of the

volume fraction of epoxy and layer thickness on such structures was determined. In summary, the highest mechanical properties were found when the volume fraction of the strong layer (TOCNF) was maximized around the 90% volume fraction, minimizing the presence of the epoxy interlayer to a 10% volume fraction. More importantly, crack digression was found to be an active mechanism of fracture retardation, increasing the toughness of some of the laminates. Even so, it was found that a weak interface adhesion led to substantial delamination, translating in a decrease of mechanical properties when the number of layers was increased (Forti et al. 2020). The research helped clear a path to the creation of stronger and tougher TOCNF laminates. It was demonstrated that by increasing the ratio between the adhesion at the interface and the cohesive strength of TOCNF layers, the crack digression mechanisms that retarded fracture while increasing the integrity of the laminates (less delamination) could be optimized. However, the effects of stronger TOCNF layers and the impact of interlayers with different mechanical properties was not addressed. Furthermore, the impact fracture behavior of laminates was still unknown.

In this study, lamination is used to investigate the role of stronger TOCNF layers, softer and stiffer interlayers, and a higher adhesion at the interface on the final properties of the layup structures. With that purpose, 4 different epoxy formulations are studied as well as a strong TOCNF + PVA composite film. The different epoxy systems are characterized and the relationship between the glass transition temperature (T_g) and storage modulus of the interlayer are studied in relationship to the mechanical properties of the final laminates. Additionally, a silane coupling agent is studied and the relationship between a stronger interface and bending, tensile, and fracture properties, are investigated. Furthermore, different fracture behaviors are associated to crack digression and interlaminar delamination within the TOCNF layers as shown by secondary electron microscopy analysis and the ratio of adhesion at the interface and the cohesive strength of the TOCNF layers. Finally, impact testing was performed on these laminates and on TOCNF films for the first time in literature.

Materials And Methods

Materials

A TOCNF suspension of 1.1 wt.% with a carboxylic content of (1.5mmol/g) was produced by USDA Forest-Service Products Laboratory (FPL), Madison, WI, USA and purchased from the University of Maine (lot #2018-FPL-CNF-129) (Saito et al. 2009). Poly(vinyl alcohol) (PVA) with a molecular weight of 146,000–186,000 g/mol and hydrolyzation percentage of 99% was bought from Sigma-Aldrich Corp, St. Louis, MO, USA.

Room temperature epoxy EpoxAcast 690™ was bought from Smooth-On, Inc, Macungie, PA, USA. Two different hardeners were used: 5-Amino- 1,3,3-trimethylcyclohexanemethyl-amine (Lot #BCCB7259), mixture of cis and trans and O,O'-Bis(2-aminopropyl) polypropylene glycol-block-polyethylene glycol-block-polypropylene glycol, better known as Jeffamine® ED-2003, Mw: 1900 (Lot #BCCB1323) and were purchased from Sigma Aldrich. A silane coupling agent, (3-Aminopropyl) triethoxysilane (APTES) 99% (Lot #MKCL4964) was also purchased from Sigma-Aldrich.

Different films were bought from McMaster including acrylonitrile butadiene styrene (ABS), low density polyethylene (LDPE), cellulose acetate, acrylic, polystyrene, aluminum, and borosilicate glass of different thicknesses.

Fabrication of Samples

TOCNF nanocomposites and films were fabricated by diluting TOCNF suspensions with deionized water to 0.53 wt%. PVA was added in a concentration of 10 wt.% (dry weight relative to TOCNF). The mix was stirred at 85°C for 2 h to promote the dissolution of the polymers in water. 40 g of the solutions were later cast into 90 mm polystyrene Petri dishes as reported in previous studies (Moon et al. 2011). The cast solutions were placed in a humidity chamber with a fixed relative humidity of 50 % at room temperature (~ 21°C). Films were completely dry after 7 days with an average thickness of $26 \pm 2 \mu\text{m}$. After drying, the films were removed from the Petri dish by cutting along the edges with a razor blade and detaching them with tape.

Laminates were fabricated following a layup method described elsewhere by the author (Forti et al. 2020). Lay-up structures were produced having 10 TOCNF layers and different epoxy interlayers with a fixed average volume fraction of epoxy of 17 ± 3 . The description of each epoxy formulation can be found in Table 1.

Table 1
Epoxy formulations. Ratios respective to epoxy resin.

Epoxy Formulation	Epoxy resin	Hardener A	Hardener B	Resin: Hardener A: Hardener B
A	EpoxAcast 690™ Part A	EpoxAcast 690™ Part B	-	100: 30: 0
B	EpoxAcast 690™ Part A	5- Amino 1,3,3-trimethylcyclohexanemethy-amine	-	100: 30: 0
C	EpoxAcast 690™ Part A	EpoxAcast 690™ Part B	O,O'-Bis(2-aminopropyl) polypropylene glycol-block-polyethylene glycol-block-polypropylene glycol Mw:1900	100: 25: 5
D	EpoxAcast 690™ Part A	EpoxAcast 690™ Part B	O,O'-Bis(2-aminopropyl) polypropylene glycol-block-polyethylene glycol-block-polypropylene glycol Mw: 1900	100: 20: 10

An adhesion promoter (APTES), used in literature to increase the compatibility between cellulose nanofibrils (CNF) and epoxy systems, was used on some of the laminates fabricated (Yeo et al. 2017). In this case, TOCNF + PVA composite films were subjected to high humidity (90 %RH) for 20 mins. After delamination, each layer was submerged in APTES for 2 mins, rinsed with ethanol and introduced to a 110°C oven for 5 mins. Lamination with epoxy would follow as described previously elsewhere (Forti et al. 2020).

Epoxy Characterization

Tensile characterization of epoxy was done by casting dogbone-shaped specimens in a silicone mold. Specimens were tested in tension using an MTS insight (MTS system Corp, Eden Prairie, MN, USA) with a 1000 N load cell and a 0.5 mm/min displacement rate. Specimens were left under low humidity chamber (25 %RH) for three days at room temperature. At least 5 specimens were tested at room temperature (24°C) and 35 % RH. Young's modulus was determined from the maximum slope of the stress-strain curve, UTS was taken as the highest point of stress before fracture and the work of failure (WOF) was calculated by integrating the area under stress-strain curve.

Dynamic Mechanical Analysis (DMA) of epoxy specimen were done by casting the different epoxy formulations into rectangular silicone molds of 37 mm x 7 mm and an average thickness of 1.5 ± 0.2 mm. Specimens were tested on a Q850 TA instruments DMA (New Castle, DE, USA), using a single cantilever clamp. Specimens were subjected to an oscillation temperature ramp from 0°C to 80°C at a 5°C/min rate, with an amplitude of 15 μ m and a frequency of 1.0 Hz. Elastic modulus (E') was taken at room temperature (24°C). T_g was reported from the E' onset, tan delta peak and the storage modulus (E') peak. Unpaired two-sample student t-tests were conducted to compare results with a threshold level set to 0.05.

Thermal characterization was performed using a differential scanning calorimetry (DSC) analyzer (Q2000 TA instruments, New Castle, DE, USA). A heating rate of 5°C/min rate was applied to the samples over a -25°C to 100°C temperature range in a nitrogen environment. Midpoint T_g 's were calculated after the heating ramp.

Laminates Characterization

Tensile testing of neat TOCNF and TOCNF + PVA composites were conducted by cutting 1:5 scale dogbone-shaped specimens using a laser cutter (Muse Hobby Laser Cutter, Full Spectrum Laser, Las Vegas, NV, USA) to obtain 1:5 scale dogbone-shaped specimens of ~ 0.8 mm width and ~ 6.5 mm of gauge length according to the ASTM D638 Standard Test Method for Tensile Properties of Plastics. Samples were tested parallel to the layer stacking in a DMA using the rate-controlled stress ramp mode fixed at a 1 N/min displacement rate. TOCNF films and composites had an average thickness of 26 ± 2 μ m. Samples were conditioned in a low humidity chamber (25% RH) for three days at room temperature before testing. A minimum of 5 specimens were tested at room temperature (24°C) and 35% RH. Unpaired two-sample student t-tests were conducted to compare results with a threshold level set to 0.05.

Laminates were tested in tension by cutting 40 mm x 4 mm rectangular shapes using a laser cutter. Fiberglass tabs were glued to the specimens using a fast cured epoxy according to the ASTM D3093 Standard Test Method for Tensile Properties Matrix Composites as described elsewhere (Forti et al. 2020). Five specimens were tested on an MTS with a 1000 N load cell and a 0.5 mm/min rate. Unpaired two-sample student t-tests were conducted to compare results with a threshold level set to 0.05.

3-point bending of the laminates was performed on a DMA by cutting 40 mm x 3 mm rectangular shapes on a laser cutter. A small flexural clamp was used at a 0.1 mm/min speed using a rate-controlled mode at room temperature (24°C) and 35% RH. 5 specimens were tested for each data point and t-tests were performed at 0.05 threshold to compare results.

Impact toughness measurements were performed on multiple polymeric films and TOCNF laminates following the ASTM D472 Standard Test Method for Total Energy Impact of Plastic Films by Dart Drop. A dart with a mass of 957g was used. A minimum of 3 samples were tested per data point.

A lap shear experiment was designed to test the adhesion at the interface between neat TOCNF films, TOCNF + PVA composites, the adhesion promoter (APTES) and the EpoxAcast 690™ (Epoxy A). The shear lap was modified from the ASTM D3164-03(2017) Standard Test Method for Strength Properties of Adhesively Bonded Plastic Lap-Shear Sandwich Joints in Shear by Tension Loading. Rectangular metal sheets (7 mm x 40 mm) x 10 mm thick were used. The films were glued into the surface of the metal using a fast-cured structural epoxy. A secondary sheet was covered with the polymer and left to cure at least 2 days. Finally, both surfaces were glued together with the same epoxy. At least 5 specimens were tested in an MTS in tension at a 1.27 mm/min rate. Failure at the interface was inspected visually and the interfacial shear strength was calculated in based of the calculated UTS and the area of bonding. Unpaired two-sample student t-tests were conducted to compare results with a threshold level set to 0.5.

Visual inspection of the laminates was performed before and after fracture. Polarized light microscopy was obtained of the side view of the laminates, by using a Carl Zeiss (Axio, Observer A1) inverted microscope in transmission mode. Polarizers were used and 10x and 20x objectives. Additionally, scanning electron microscopy (SEM) were taken of the side views of fracture specimens. A Phenom SEM (FEI Company, Hillsboro, OR, USA) was used for this purpose. Samples were coated with platinum for about 45 s inside an Emitech, K550X Sputter coater (Quorum Technologies Ltd., East Sussex, UK).

Finally, optical absorbance (UV-Vis spectroscopy Spectramax Plus 384, Molecular devices Corp., Sunnyvale, CA) of neat TOCNF, TOCNF + PVA composites and laminated samples were measured and compared against borosilicate glass. A wavelength of 400 nm to 750 nm range was used with air as a background. Data was normalized by the sample thickness for comparison purposes.

Results And Discussion

Processing

A hand lay-up method was used to fabricate the different sets of laminates following a procedure described in detail in a previous publication (Forti et al. 2020). A total of four epoxy formulations (described in the materials and methods section) with different mechanical properties were used as interlayers for the laminates. All samples maintained the transparency and low haziness of the original TOCNF layers as shown in Fig. 1 and Figure SI1 (supplemental information), although a few bubbles and dirt specks are visible. Characteristic plots of transmittance are shown in Figure SI2 where different lay-up structures are compared against borosilicate glass.

Flexural properties

The mechanical properties of the laminates were evaluated via bending on a DMA. All the laminates tested were comprised of 10 layers of neat TOCNF or TOCNF + PVA composite films and different epoxy interlayers. The volume fraction of epoxy was fixed at 17 ± 3 % out of the total laminate to isolate the effect of the interlayer in the mechanical properties of the laminate. Results showing the different laminates tested are presented in Fig. 2. Information about the different epoxy formulations can be found on Table 1.

The percentage change of each laminate in relationship to the neat TOCNF - epoxy A laminate (red bar) is expressed in the charts. Each laminate system will be analyzed by isolating the effect of different components during the discussion, progressing from the smaller demarked square on the plot (Fig. 2) to the biggest one.

Influence of TOCNF layers

The first square (smallest) correlates to the increase achieved by replacing neat TOCNF films with a TOCNF + PVA composite film. In a previous study performed by Forti et al. (2021), the introduction of PVA at a low level of 10wt% (relative to the dry weight of TOCNF) as a reinforcing agent in hypochlorite TOCNF films was described. The mechanical increases achieved in tension were reported to be around the 48% in Young's modulus, 93% in UTS and 165% in WOF when compared with the neat TOCNF (Endrina S. Forti, Sami M. El Awad Azrak, Xin Y. Ng, Whirang Cho, Gregory T. Schueneman, Robert J. Moon, Douglas M. Fox 2021). The results shown in Fig. 2 show increases of flexural strength of 29%, bending modulus of 50% and WOF of 25% when the same layers were introduced in the laminate. The increased tensile properties of TOCNF + PVA layers did not translate into the same proportion of increase in bended laminates, which is expected. While TOCNF + PVA films are the main component in the laminated samples, they do not constitute 100% of it. Only 80% volume fraction will follow the behavior of the TOCNF composite while the remaining is expected to follow the performance of the epoxy interlayer. This notion is well understood and described by the rule of mixtures of laminated materials in tension. Additionally, there is not a straight relationship between tension and bending properties of inhomogeneous materials. This conception lies in the fact that most materials do not exhibit the same moduli in tension as in compression. When a laminated material is bent, some of the layers will strain and others will constrain, making the comparison between tension and bending properties difficult (Jones and Morgan 1980). Hence, since the bending behavior of TOCNF + PVA films is difficult to account for (not enough thickness) and the relationship between the rule of mixtures of tensile and bending of

materials is not direct, it is difficult to predict the magnitude of increases that should have been achieved by replacing the neat TOCNF layers with the stronger TOCNF + PVA composite films. Nevertheless, when accounting for the generation of extra interlaminar stresses generated by the mismatch between the mechanical properties of TOCNF and epoxy, it is safe to say that an increase of ~ 25% across diverse mechanical properties when a 17 vol% of epoxy is introduced is a good indication of the role of the stronger composite in the bending behavior of the laminates. To get an additional understanding of the differences between the two laminates, SEM pictures were taken after bending and are presented in Fig. 3

The fracture behavior of the two set of laminates (neat TOCNF and TOCNF + PVA) show some relevant differences, especially when looking closer into the behavior of TOCNF + PVA layers. To highlight such differences a scheme is presented in Fig. 3. In general, laminates with neat TOCNF layers showed widespread interfacial delamination, which is understood as the debonding of the TOCNF film from the interface (epoxy). In contrast, TOCNF + PVA films induced a secondary type of crack retardation mechanism known in literature as interlayer delamination (called here “intralayer damage” to avoid confusion). In general, a single TOCNF film, when dried, is constituted of a stack of many individual layers (1 μm or less in thickness), and it is between these layers that the intralayer damage occurs. In failure, the nucleation of cracks within the single TOCNF films is the result of the combined effect of:

1. The random in-plane orientation of the fibrils
2. The stronger intralaminar fibrils interactions compared to the weaker interlaminar bonding.

Consequently, intralayer damage takes advantage of the weaker interlaminar interactions, nucleating new surfaces in between the stack of layers within a single TOCNF film. The nucleation of such surfaces is an important energy dissipation mechanism of fracture retardation that increases the toughness of laminates, and will be discussed extensively during this study (Moon et al. 2011).

Influence of epoxy formulation

Usually, lay-up structures are constituted by strong or stiff materials that are laminated with a very ductile interlayer to maximize properties. The ductile interlayers are usually in a lower volume percentage when compared to the strong material. Even so, a ductile interlayer plays a significant role in increased work of fracture due to the introduction of different mechanisms for fracture retardation (Cook et al. 1964; Cepeda-Jiménez et al. 2008).

In this study, different epoxy systems were analyzed to further investigate the impact of ductile vs stiff epoxy layers in the mechanical properties of the laminates. For the different epoxy systems formulated, Fig. 4 shows the T_g as measured by DMA and DSC analysis, while Fig. 5 shows the storage modulus as measured by DMA.

In general, the glass transition temperature in polymers is related to medium to long range motion of the polymer chain, therefore, it is defined as a function of chain stiffness/length and it is inversely proportional to the free volume in the polymeric network (Gibbs and Dimarzio 1958; Hagen et al. 1994). In this study, the T_g of the different epoxy systems was measured through DMA and DSC. Dynamic

measurements were performed with a single cantilever clamp at a fixed frequency and amplitude. The T_g was taken from the onset of the storage modulus, the peak of the loss modulus and the tan delta as the materials were deformed in a sinusoidal deformation. Each of these measurements is related to a specific set of events within the polymeric chains. The onset of E' occurs at the lower temperature when compared with the loss modulus peak and the tan delta. This temperature is usually understood as the onset of the decrease in mechanical properties in polymers, which is why it is relevant from a mechanical properties standpoint. The loss modulus peak is extensively related to molecular processes and it denotes the molecular movements happening at the medium and long range in the polymeric chain. Finally, tan delta occurs at the highest temperature as it is defined as the middle point between the rubbery and glassy state of the polymer (Instruments; Hagen et al. 1994). DSC measurements were also conducted on all the samples, and T_g was reported as the middle point of the slope during a heat cycle (Wendlandt and Gallagher 1981). Overall, all measurements showed a higher T_g for the epoxy B when compared with A. Furthermore, epoxies C and D had a lower T_g , where epoxy C showed higher transition temperatures than epoxy D (i.e. $B > A > C > D$). It is important to highlight that T_g values are reported from different techniques only for comparison purposes. It is the assumption of the authors that the T_g measured from the onset of E, has a higher importance in the mechanical properties of the laminates, influencing the modes of fracture in the specimens (i.e. before T_g fracture behavior is independent of temperature)(Fernandes et al. 2016).

It is expected that by replacing the hardener of the initial epoxy formulation (epoxy A), described by the manufacturer as "Polyoxypropylenediamine" for one such as 5- Amino 1,3,3-trimethylcyclohexanemethylamine (refer to Figure SI3 of the supplemental information for the molecular structure) will result in an increased stiffness of the crosslinked structure, translating in a higher T_g and storage modulus but also in some brittleness in the resin. On the other hand, a longer and more ductile hardener such as O,O'-Bis(2-aminopropyl) polypropylene glycol-block-polyethylene glycol-block-polypropylene glycol (Figure SI4 of the supplemental information) with a relatively high molecular weight (i.e. M_w : 1900 g/mol) will introduce more space between crosslinks in the resin, making it more flexible and susceptible to movement at lower temperatures (therefore the lower T_g and storage modulus). This is true for epoxies C and D, where the original hardener of the epoxy was mixed with the high molecular weight hardener in two different proportions, resulting in lower values of T_g and moduli when compared with epoxy A.

Figure 2 shows the influence of such resins on laminate properties, where the second square highlights the results. Overall, the introduction of a stiffer resin (epoxy B), decreased the mechanical properties of the TOCNF + PVA laminates with the epoxy A resin, reversing the 29% flexural strength increase achieved by the introduction of stronger TOCNF + PVA layers. Furthermore, Young's modulus and WOF showed no statistical difference when compared against TOCNF + PVA – epoxy A laminate. Considering epoxy C, a somewhat more ductile interlayer (20% decrease in elastic modulus when compared to epoxy A), there is no statistical difference with regards to epoxy A with the TOCNF + PVA laminate for modulus, flexural strength or WOF. However, a continued increase in the epoxy ductility (e.g., lower T_g and elastic modulus)

by using epoxy D, translated into a degradation of the strength, a large reduction of the bending modulus but an increase in the WOF of the laminate. Thus, as the epoxy interlayer ductility increased (e.g., stiffness decreased) there seems to be a threshold before which the epoxy makes little difference, but beyond which it reduces stiffness and strength, and increases WOF.

When examining the fracture behavior of the laminates in Fig. 6 it is evident that different modes of fracture are being introduced depending on interlayer stiffness. Overall, the trend seems to highlight an intralayer damage within the TOCNF + PVA layers when introducing a stiffer interlayer (epoxy B), that changes into an interfacial delamination when a softer interlayer is in place (epoxy D). This behavior might be triggered by the difference in modulus between the strong layers (TOCNF + PVA) and the epoxy. When this difference is higher, as is the case with epoxy D that is more ductile, the amount of interfacial shear stress between the two materials can lead to increased delamination at the surface between the two (i.e. interfacial delamination). As this difference is reduced (by introducing stiffer epoxies) the shear stresses at the interface are reduced and the intralayer damage within TOCNF layers is more evident. Nevertheless, it seems like resins with a set of properties between the two extremes performed best. In this particular case, epoxy A and epoxy C behaved better in terms of increased flexural strength, moduli and WOF in the laminates. Figure 6 (c) shows the fracture of TOCNF + PVA laminate with epoxy C, where extensive delamination and intralayer damage can be appreciated. Therefore, the increased mechanical properties might be attributed to a combined effect of the two different fracture retardation mechanisms at play. As such, having a soft enough epoxy to promote interlayer delamination, but stiff/strong enough to allow intralayer damage to balance the stresses of the two modes seems ideal.

Influence of a silane coupling agent

In a previous work by Forti et al. (2020) the adhesion at the interface of TOCNF + epoxy A laminates was found to be lower than desired when compared to the cohesive strength of neat TOCNF layers (Forti et al. 2020), suggesting a potential mechanism for improvement. By increasing interfacial adhesion between TOCNF and epoxy, the laminates could improve their performance in mechanical loading, while also sustaining beneficial crack stop mechanisms such as crack digression.

To study how the level of adhesion at the interface between TOCNF and epoxy affects the mechanical properties of laminates, a silane coupling agent was added to a TOCNF + PVA – epoxy A system. The reasoning behind this can be found in literature, where silane coupling agents have been used to increase the compatibility of CNFs with different materials. In general, silane coupling agents serve as a bridge between two substrates, introducing ionic or covalent bonds between them and in doing so an increase in the overall adhesion (P lueddemann 1970). In the specific case of CNFs and epoxy, APTES, a silane coupling agent with an amine active group that can easily react with epoxy, phenolics and polyesters has been previously studied (Rol et al. 2019). For example, Yeo et al. (2017) modified CNF fibrils with APTES to achieve a 1.5–2.2 times higher mechanical properties of the epoxy reinforced with the modified APTES- CNF (Yeo et al. 2017). Therefore, APTES was introduced in this study as an adhesion promoter.

To demonstrate the effect of APTES on adhesion, a contact angle study was completed on TOCNF + PVA films that were clear of visible defects. Figure SI5 of supplemental information shows the change in the contact angle after applying APTES to TOCNF + PVA films. Overall, TOCNF + PVA films exhibit a static contact angle of $70 \pm 3^\circ$ that was increased to $100 \pm 5^\circ$ after treatment with APTES, which is in line with previous APTES modification studies. Lu et al. (2008) achieved a change in the water contact angle of CNF from 15° to 90° without imparting any changes in the crystalline structure of CNF. In general, CNFs are rich in hydroxyl groups (OH) making them hydrophilic in nature (Lu et al. 2008). While it can be expected that TOCNF may be somewhat different than CNFs due to the conversion of some of the OH groups to COONa, it will still retain a similar hydrophilic behavior thanks to the large amount of unconverted OH groups on the surface. Further, while many expect the amine surface to of APTES to be relatively hydrophilic, APTES tends to interact with hydrogen bonding groups underneath (such as alcohol or silanol) and push the propyl segment towards the top, giving a relatively hydrophobic surface (please refer to Figure SI6 for the molecular structure of APTES) (Malekzadeh and Zhang Newby 2020).

Overall, a higher adhesion at the interface was achieved by the introduction of APTES as can be seen in the lap shear results exhibit on Table 2, where for both neat TOCNF and TOCNF composite films with epoxy A the results did not show a statistical difference. In contrast, when APTES was added, the peak stress increased by 47% while the strain before failure increased by 86%. This confirms the authors hypothesis that by achieving a surface treatment on the films through a hydrolysis-condensation reaction, a bridge between TOCNF and epoxy was achieved (Figure SI7) resulting in a higher adhesion as shown by the data presented.

Table 2
Lap shear results on different TOCNF and TOCNF + PVA composites and adhesion promoters.

Material A	Material B	Adhesion Promoter	Peak Stress (MPa)	Peak Strain (mm/mm)	Failure
TOCNF	Epoxy A	-	3.6 ± 0.5	0.008 ± 0.001	Interface
TOCNF + 10wt% PVA	Epoxy A	-	3.8 ± 0.9	0.008 ± 0.005	Interface
TOCNF + 10wt% PVA	Epoxy A	APTES	5.6 ± 0.4	0.015 ± 0.005	Interface

The measurement of the adhesion at the interface is important to understand crack digression mechanisms on the laminates. Overall, the adhesion between the interfaces of a laminate is vital and defines the behavior of nucleated cracks and their relation to the delamination behavior of laminates. In general, one of the main attributes that affects the propagation speed of a crack in a laminated material is the adhesion at the interface. To name an example, in homogenous brittle materials, once a crack is initiated, it will propagate through the material rapidly causing fracture. One can then infer that if the adhesion between the two interfaces in a laminate is sufficiently high, once a crack is nucleated, it might

go through all the layers without perceiving the presence of an interface. In the opposite case (i.e. if the adhesion between the two is weak), the crack might diverge along the interface, increasing the overall toughness of the laminate, but causing early delamination and compromising the overall strength. However, there is an ideal scenario where the adhesion is weak enough to provoke the diversion of a crack but strong enough not to weaken the specimen. This case for purely brittle materials has been defined in literature by a ratio, if the interface adhesion in a laminate is less than 0.35 times the cohesive strength of the strong material in the laminate, then cracks can be diverted but the laminate will retain some of its inheriting strength (Cook et al. 1964; Kendall 1975; Chellappa and Jang 1996; Forti et al. 2020).

In the particular case of neat TOCNF laminates, it was shown in a previous publication that this value was around 0.03, suggesting there was room for potential improvements (Forti et al. 2020). Table 3 shows the same ratio calculated for different configurations of TOCNF composites with regards to epoxy A. To calculate such ratios, tensile testing of neat TOCNF and TOCNF + PVA films was performed via DMA. For the specific case of TOCNF + PVA + APTES films, the same value of UTS of the TOCNF + PVA composite film was assumed, since APTES does not disrupt the structure of the TOCNF layers (Lu et al. 2008).

Table 3

UTS properties of Neat TOCNF and TOCNF + PVA films. TOCNF + PVA + APTES films are assumed to have the same UTS as TOCNF + PVA layers. Adhesion / Cohesive strength ratio for different TOCNF configurations. Adhesion measured in relation to Epoxy A.

Films	UTS (MPa)	Adhesion (MPa)	Ratio Adhesion/UTS (MPa/MPa)
Neat TOCNF	151 ± 11	3.6 ± 0.5	0.024
TOCNF + PVA	256 ± 12	3.8 ± 0.9	0.015
TOCNF + PVA + APTES	256 ± 12	5.6 ± 0.4	0.022

As can be seen in Table 3 the original ratio of 0.024 was reduced to 0.015 when TOCNF + PVA layers were incorporated to laminated specimens. This is due to the higher cohesive strength achieved by adding PVA to TOCNF layers. Without an adhesion promoter, the adhesion at the interface remained the same and the ratio was reduced. To further investigate how this ratio affected the mechanical properties of the laminates, a set of 3 different laminates were prepared and measured in tension. Results are presented in Fig. 7.

Tensile testing results show a different tendency for laminates with TOCNF + PVA composite films versus those made with neat TOCNF layers. Overall, laminates with TOCNF + PVA composites performed better due to the larger strength of the individual layers. Nonetheless, it seems like without an adhesion promoter such as APTES (open blue triangle marker) the UTS values in tension are not reaching the idealized performance predicted by the rule of mixtures. This behavior may be due to the increased

difference in performance between TOCNF + PVA layers and epoxy A. When the difference in mechanical properties grows larger, the mismatch in Young's modulus between the strong layers and the epoxy produces an increased shear stress when the material is stretched in tension (Herakovich 1981; Kant and Swaminathan 2000). It is believed by the authors that the high shear stresses generated by the mismatch of mechanical properties, in addition to the decreased adhesion ratio in the interface, generates extensive delamination and an improper transmission of the load between the layers. When APTES was added (closed blue triangle marker) an increased adhesion was achieved, resulting in an improved tensile strength of the laminate, that is closer to the expected values (dictated by the rule of mixtures).

Finally, the flexural properties of the APTES laminates were measured and compared to the Neat TOCNF and TOCNF + PVA laminates. Results are shown in Fig. 2 and are highlighted by the biggest square in the plots. Data shows an increase of 25% in the flexural strength, 30% in bending modulus and a reduction of 25% in WOF properties attributed to the increased interfacial adhesion (taken from the straight comparison between TOCNF + PVA laminates with epoxy A interlayers). When compared to the original non-PVA laminate (red bar in the plots), an increase of 80% in flexural strength, 61% in bending modulus and approximately the same WOF was obtained, showing that both improved TOCNF strong phase and adhesion can lead to large increases in properties. Nonetheless, even when a much higher mechanical performance was achieved, the adhesion ratio of the samples is still low. Therefore, there may be still room for improvement, in fact, it is believed by the authors that achieving a higher adhesion between the TOCNF + PVA composites and the epoxy is crucial to decrease the delamination behavior of laminates while increasing the its overall performance.

Impact rupture energy

Both 3-point bending, and tensile testing involves the deformation of specimens to the point of fracture while increasing the load applied. While both techniques offer a wide range of information about the overall mechanical response of a specimen, they do not predict the fracture behavior of specimens under a moderate or high velocity blunt impact. Systems where a strong material is laminated with a ductile material have been shown to produce high toughness materials when the conditions are appropriate (i.e. an adequate combination of moduli, good adhesion, appropriate interlayer thickness and sufficient number of layers). A good example of this combination can be found in ballistic glass (glass with polyvinyl butyral or other polymers as interlayer(Martín et al. 2020)), where the match of the right properties produce a material capable of resisting impacts at high velocity (Shim et al. 2016). This type of study, necessary to predict the toughness capabilities of our system has not been done before on TOCNF materials and it is important to fully understand the behavior of the laminates under a wider range of conditions. Some of the most popular impact studies include techniques like Charpy and Izod where the material is notched and subjected to a high strain-rate impact. In this study, a free-falling dart test was used as it is a common impact test performed on thin films that are usually targeted for packaging applications, a field of interest for the cellulose community. The method is highly sensitive to thickness, making it hard to derive straight relationships between the energy to rupture and the thickness of different materials. Further, a complete rupture of the films is necessary to make the calculations

possible, which limits the spectrum of materials that can be tested. Hence, only films with similar thicknesses were tested as a comparison point for cellulose materials (both films and laminates).

A set of three different laminates were prepared and subjected to drop dart testing along with other common materials. 10-layer neat TOCNF – epoxy A, TOCNF + PVA – epoxy A, and TOCNF + PVA + APTES – Epoxy A were selected for the testing to analyze how different TOCNF composites and adhesion promoters could change the response of the laminates. Other common polymers within similar thicknesses and toughness such as ABS, known as an engineering polymer with excellent toughness (Olivera et al.), LDPE, a common polymer used in the film industry due to its cheap price and great toughness (Jordan et al. 2016), cellulose acetate, used in a wide range of products including films for packaging applications (Puls et al. 2011), acrylic (PMMA), known as a good alternative to replace glass (Penzel 2000), high impact polystyrene (HIPS) (J. R. Wünsch 2000, p. 15), aluminum and borosilicate glass (Axinte 2011), extensively used in industry due to its higher resistance to thermal shock were tested. Results are presented in Fig. 8 where the energy to rupture was divided by thickness as rupture energy scales by the volume deformed and normalized by density to plot against the tensile specific strength of each material in an “Ashby” style plot to compare the materials.

Results show a highlighted area for each group of materials studied. The blue bubble represents ductile polymers with an overall low specific strength but high specific rupture energy. ABS exhibited the highest specific energy to rupture, as expected as it is an engineering polymer, composed by acrylonitrile and butadiene (a synthetic rubber), which allows for a good chemical and thermal stability while also sustaining high toughness (Olivera et al.). Acrylic in the other hand, showed a low specific rupture energy but higher specific strength, which is not uncommon due to its amorphous nature (Penzel 2000). In comparison, laminates showed a similar toughness to acrylic, with a much higher specific strength. Finally, borosilicate glass and TOCNF and its laminates are shown in the low specific energy / high specific strength area of the plot (red bubble). While glass was expected to behave in a brittle manner (low toughness) the glass tested here was thin (i.e. characteristic strength goes up as size goes down) which explains the higher toughness exhibited (Shand 1965).

Single TOCNF films need some elaboration as this is the first report to date of falling dart impact testing of these materials. Neat TOCNF films showed strength to failure similar to borosilicate glass with a higher specific energy to rupture. The composite films (TOCNF + PVA) showed a higher specific strength but a reduced energy to rupture when compared to Neat TOCNF films. Overall, impact testing shows that TOCNF has great potential as a high strength transparent or structural material as when a small amount of PVA enhancer is added it can achieve similar specific impact energy to rupture to acrylic and aluminum, but almost 3 times and 7 times higher specific strength of each, respectively.

Neat TOCNF laminates performed similarly to its respective unlaminated single films and to borosilicate glass. As the TOCNF laminate is much higher in strength than typical polymers but still fails in a brittle manner, this is expected. While TOCNF + PVA -epoxy A laminate shows lower strength than the single film, its impact performance seems to be increased with lamination, indicating toughening mechanisms

attributed to the interfaces. Regardless, TOCNF + PVA -epoxy A performed better in terms of energy of rupture than either the glass or neat TOCNF laminate. In comparison, the laminate with an increased adhesion (APTES laminate) underperformed, reaching the same level than the original laminate (Neat TOCNF laminate) while showing a higher specific strength. This might find a good explanation in the crack digression mechanism exhibited by all the laminates. As discussed previously, the ratio between the interface adhesion and the cohesive strength of the material dictates the degree of crack digression that a system will experienced upon fracture. The lower this value is, the higher the crack digression in the system, leading to delamination but also a great degree of energy absorption as the crack deflects to an unfavorable direction, prolongating its path across the laminate, resulting in higher toughness (Feng et al. 2000). Therefore, the results shown in Fig. 8 are in agreement with the ratios calculated in Table 3 where the TOCNF + PVA laminate shows the smaller adhesion/strength ratio (0.015), translating into a higher toughness. This was also corroborated by the three-point bending results, where this laminate showed the higher WOF just as both neat TOCNF and APTES laminates showed the same value of WOF, adhesion ratio, and energy to rupture. Overall, while the laminates fracture in a brittle way when compared to ductile polymers (ABS, LDPE and acetate), the specific impact rupture energy of the laminates is similar or higher than that of other transparent structural materials such as glass and acrylic, yet with a significantly higher specific strength allowing for the potential of weight savings by using less material to accomplish a similar function.

Conclusions

Transparent TOCNF-epoxy laminates were fabricated and tested to determine how the strong layer properties, epoxy interlayer properties, and strength of adhesion between the strong layer and the epoxy affected the overall laminate mechanical properties. 3-point bending results showed a strong relationship between the presence of stronger layers (TOCNF + PVA) with a higher flexural strength, bending modulus and WOF. Overall, a stiffer epoxy generated a diminished UTS and flexural modulus and substantial intralayer damage. On the other hand, a more ductile epoxy increased the WOF of the laminates, inducing a higher delamination at the interfaces. The delamination mechanism was attributed to the strong mismatch between the properties of TOCNF + PVA composites and the epoxy. Results highlighted a better mechanical performance when laminates were fabricated with an intermediate, i.e. not too stiff or too ductile interlayer, and were able to exhibit both delamination at the interface and intralayer damage as a fracture behavior mechanism. The addition of a silane coupling agent (APTES) to the TOCNF – PVA laminates increased the adhesion at the interface, resulting in a higher UTS when tested in tension and a reduced energy to rupture associated with the reduction of crack digression mechanisms in the system. In general, laminates with strong TOCNF layers (TOCNF + PVA) and APTES, increased the flexural strength (+ 61%) and bending modulus (80%) while retaining the same WOF. Finally, for the first time, impact testing of TOCNF was performed. The specific impact rupture energy of the laminates was comparable to or slightly higher to those achieved by acrylic polymers and borosilicate glass while maintaining a similar or higher specific strength to glass. Additionally, laminates showed an excellent transparency and low haziness to the naked eye.

SUPPORTING INFORMATION

The following files are available free of charge:

- Picture of a 10-layer TOCNF + PVA – epoxy A laminate, showing high transparency and low haziness. (PDF)
- Visible transmittance via UV-Vis spectroscopy of TOCNF laminates, and borosilicate glass. (PDF)
- Scheme of interfacial vs interlayer delamination for a TOCNF -epoxy laminate. (PDF)
- Molecular structure of hardener 5- Amino 1,3,3-trimethylcyclohexanemethy- amine introduced to formulation B. (PDF)
- Molecular structure of hardener O,O'-Bis(2-aminopropyl) polypropylene glycol-block-polyethylene glycol-block-polypropylene glycol used on formulation C and D. (PDF)
- Molecular structure for APTES (3-Aminopropyl) triethoxysilane. (PDF)
- Static contact angle photographs of water droplets in different substrates. (a). TOCNF + PVA composite and TOCNF + PVA modified with APTES. (PDF)
- Schematic of the surface modification achieved of TOCNF with APTES. (PDF)
- Microscopy of 10-layer TOCNF or TOCNF + PVA composite laminates after 3-point bending fracture. (PDF)
- SEM of fracture behavior after free dart impact of 10-layer laminates. (PDF)

Declarations

ACKNOWLEDGEMENTS

The authors would like to acknowledge financial support from the Private–Public Partnership for Nanotechnology in the Forestry Sector (P3Nano) under Grant Number 109217.

Author Contributions

The manuscript was written through the contributions of all authors. All authors have approved the final version of the manuscript.

Ethics declarations

The author declares no conflict of interest, financial or otherwise. All authors have consented to publication. No human or animal subjects were involved in this study. The study meets all relevant ethical standards and approvals.

References

Axinte E (2011) Glasses as engineering materials: A review. *Mater. Des.* 32:1717–1732

- Benítez AJ, Walther A (2017) Cellulose nanofibril nanopapers and bioinspired nanocomposites: A review to understand the mechanical property space. *J. Mater. Chem. A* 5:16003–16024
- Cepeda-Jiménez CM, Pozuelo M, Ruano OA, Carreño F (2008) Influence of the thermomechanical processing on the fracture mechanisms of high strength aluminium/pure aluminium multilayer laminate materials. *Mater Sci Eng A* 490:319–327. <https://doi.org/10.1016/j.msea.2008.01.034>
- Chellappa V, Jang BZ (1996) Crack growth and fracture behavior of fabric reinforced polymer composites. *Polym Compos* 17:443–450. <https://doi.org/10.1002/pc.10632>
- Clarkson CM, El Awad Azrak SM, Forti ES, et al (2020) Recent Developments in Cellulose Nanomaterial Composites. *Adv Mater* 2000718. <https://doi.org/10.1002/adma.202000718>
- Cook J, Gordon JE, Evans CC, Marsh DM (1964) A Mechanism for the Control of Crack Propagation in All-Brittle Systems. *Proc R Soc London Ser A, Math Phys Sci* 282:508–520
- Endrina S. Forti, Sami M. El Awad Azrak, Xin Y. Ng, Whirang Cho, Gregory T. Schueneman, Robert J. Moon, Douglas M. Fox JPY (2021) Mechanical Enhancement of Cellulose Nanofibril (CNF) Films Through the Addition of Water-soluble Polymers. *Cellulose*
- Feng QL, Cui FZ, Pu G, et al (2000) Crystal orientation, toughening mechanisms and a mimic of nacre. *Mater Sci Eng C* 11:19–25. [https://doi.org/10.1016/S0928-4931\(00\)00138-7](https://doi.org/10.1016/S0928-4931(00)00138-7)
- Fernandes RL, De Moura MFSF, Moreira RDF (2016) Effect of temperature on pure modes I and II fracture behavior of composite bonded joints. *Compos Part B Eng* 96:35–44. <https://doi.org/10.1016/j.compositesb.2016.04.022>
- Forti ES, Moon RJ, Schueneman GT, Youngblood JP (2020) Transparent TEMPO oxidized cellulose nanofibril (TOCNF) composites with increased toughness and thickness by lamination. *Cellulose* 1–17. <https://doi.org/10.1007/s10570-020-03107-8>
- Fujisawa S, Okita Y, Fukuzumi H, et al (2011) Preparation and characterization of TEMPO-oxidized cellulose nanofibril films with free carboxyl groups. *Carbohydr Polym* 84:579–583. <https://doi.org/10.1016/j.carbpol.2010.12.029>
- Gibbs JH, Dimarzio EA (1958) Viscous Liquids and the Glass Transition: A Potential Energy Barrier Picture. *J Chem Phys* 28:3728. <https://doi.org/10.1063/1.1744141>
- Hagen R, Salmén L, Lavebratt H, Stenberg B (1994) Comparison of dynamic mechanical measurements and Tg determinations with two different instruments. *Polym Test* 13:113–128. [https://doi.org/10.1016/0142-9418\(94\)90020-5](https://doi.org/10.1016/0142-9418(94)90020-5)
- Herakovich CT (1981) On the Relationship between Engineering Properties and Delamination of Composite Materials. *J Compos Mater* 15:336–348. <https://doi.org/10.1177/002199838101500404>

Instruments T Measurements of the Glass Transition Temperature Using Dynamic Mechanical Analysis. <https://www.tainstruments.com/pdf/literature/TS64.pdf>. Accessed 28 Feb 2021

Isogai A, Saito T, Fukuzumi H (2011) TEMPO-oxidized cellulose nanofibers. *Nanoscale* 3:71–85. <https://doi.org/10.1039/C0NR00583E>

1. R. Wünsch (2000) *Polystyrene: Synthesis, Production and Applications* - J. R. Wünsch - Google Books

Jones RM, Morgan HS (1980) Bending and extension of cross-ply laminates with different moduli in tension and compression. *Comput Struct* 11:181–190. [https://doi.org/10.1016/0045-7949\(80\)90157-1](https://doi.org/10.1016/0045-7949(80)90157-1)

Jordan JL, Casem DT, Bradley JM, et al (2016) Mechanical Properties of Low Density Polyethylene. *J Dyn Behav Mater* 2:411–420. <https://doi.org/10.1007/s40870-016-0076-0>

Kant T, Swaminathan K (2000) Estimation of transverse/interlaminar stresses in laminated composites – a selective review and survey of current developments. *Compos Struct* 49:65–75. [https://doi.org/10.1016/S0263-8223\(99\)00126-9](https://doi.org/10.1016/S0263-8223(99)00126-9)

Kendall K (1975) Transition between Cohesive and Interfacial Failure in a Laminate. *Proc R Soc A Math Phys Eng Sci* 344:287–302. <https://doi.org/10.1098/rspa.1975.0102>

Lu J, Askeland P, Drzal LT (2008) Surface modification of microfibrillated cellulose for epoxy composite applications. *Polymer (Guildf)* 49:1285–1296

Malekzadeh E, Zhang Newby BM (2020) Thermoresponsive Poly(vinyl methyl ether) (PVME) Retained by 3-Aminopropyltriethoxysilane (APTES) Network. *ACS Biomater Sci Eng* 6:7051–7060. <https://doi.org/10.1021/acsbiomaterials.0c01376>

Martín M, Centelles X, Solé A, et al (2020) Polymeric interlayer materials for laminated glass: A review. *Constr. Build. Mater.* 230:116897

Moon RJ, Martini A, Nairn J, et al (2011) Cellulose nanomaterials review: structure, properties and nanocomposites. *Chem Soc Rev* 40:3941–3994. <https://doi.org/10.1039/C0CS00108B>

Olivera S, Muralidhara HB, Venkatesh K, et al Plating on acrylonitrile–butadiene–styrene (ABS) plastic: a review. *J Mater Sci* 51:3657–3674. <https://doi.org/10.1007/s10853-015-9668-7>

P lueddemann EP (1970) Adhesion Through Silane Coupling Agents. *J Adhes* 2:184–201. <https://doi.org/10.1080/0021846708544592>

Penzel E (2000) Polyacrylates. In: *Ullmann's Encyclopedia of Industrial Chemistry*. Wiley-VCH Verlag GmbH & Co. KGaA, Weinheim, Germany

Puls J, Wilson SA, Hölter D (2011) Degradation of Cellulose Acetate-Based Materials: A Review. *J. Polym. Environ.* 19:152–165

Rol F, Belgacem MN, Gandini A, Bras J (2019) Recent advances in surface-modified cellulose nanofibrils. *Prog. Polym. Sci.* 88:241–264

Saito T, Hirota M, Tamura N, et al (2009) Individualization of Nano-Sized Plant Cellulose Fibrils by Direct Surface Carboxylation Using TEMPO Catalyst under Neutral Conditions. *Biomacromolecules* 10:1992–1996. <https://doi.org/10.1021/bm900414t>

Shand EB (1965) Strength of Glass—The Griffith Method Revised. *J Am Ceram Soc* 48:43–49. <https://doi.org/10.1111/j.1151-2916.1965.tb11791.x>

Shim GI, Kim SH, Ahn DL, et al (2016) Experimental and numerical evaluation of transparent bulletproof material for enhanced impact-energy absorption using strengthened-glass/polymer composite. *Compos Part B Eng* 97:150–161. <https://doi.org/10.1016/j.compositesb.2016.04.078>

Wendlandt WW, Gallagher PK (1981) Instrumentation. In: *Thermal Characterization of Polymeric Materials*. Elsevier, pp 1–90

Yeo JS, Kim OY, Hwang SH (2017) The effect of chemical surface treatment on the fracture toughness of microfibrillated cellulose reinforced epoxy composites. *J Ind Eng Chem* 45:301–306. <https://doi.org/10.1016/j.jiec.2016.09.039>

Figures



Figure 1

Picture of a 10-layer TOCNF + PVA + APTES and epoxy A laminate, showing high transparency and low haziness.

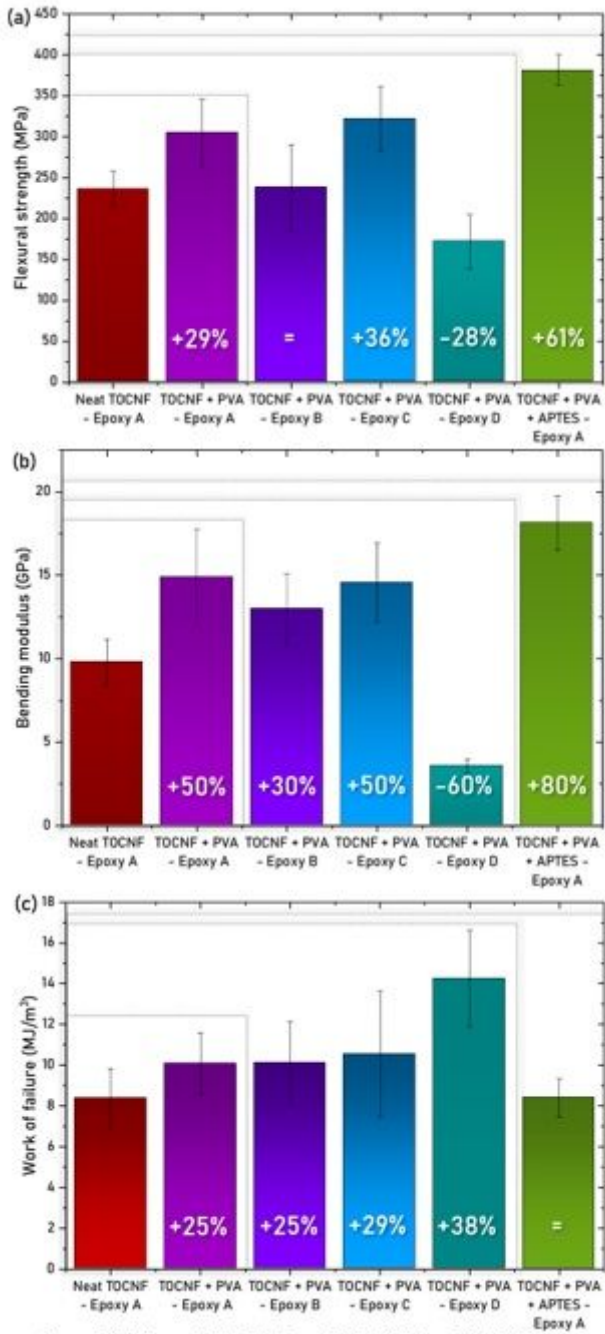


Figure 2

Flexural properties of 10-layer TOCNF and TOCNF + PVA laminates. (a) Flexural strength (MPa). (b) bending modulus (GPa) and (c) Work of failure (MJ/m³). The first square (from smallest to biggest) highlights the influence of stronger TOCNF layers, the second, the influence of different epoxies, the biggest, highlights the effect of an increased adhesion. Numbers represent the increase when compared to the reference sample (Neat TOCNF – Epoxy A / red column), = means no statistical difference between the samples.

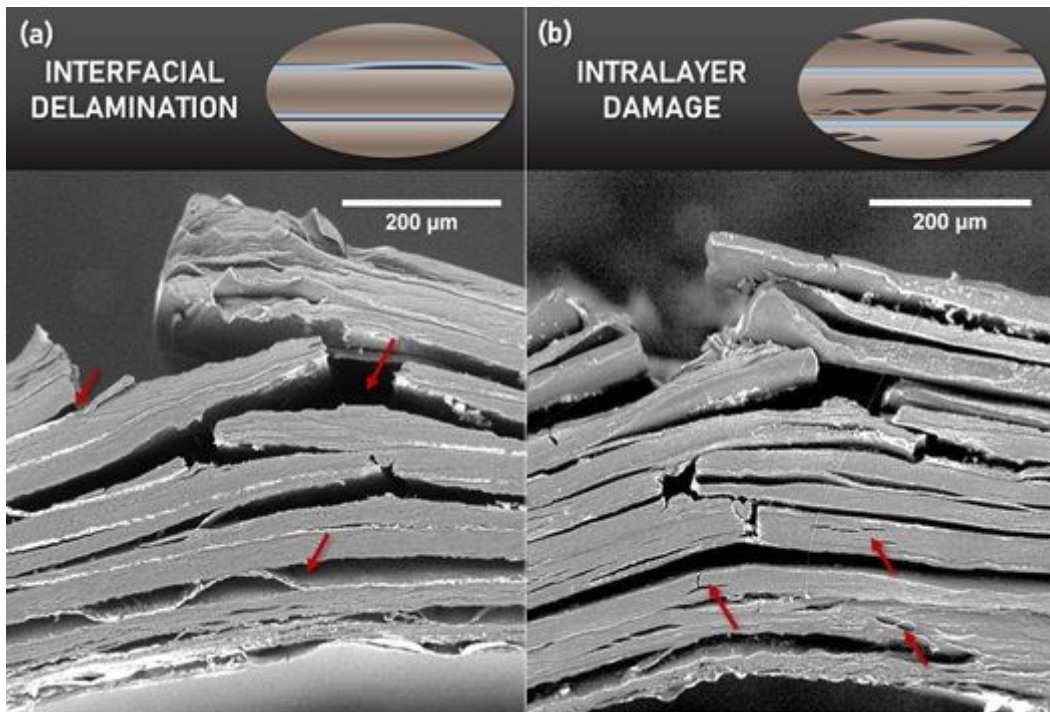


Figure 3

SEM images of the fracture behavior of 10-layer TOCNF film laminates. (a) Neat TOCNF – Epoxy A laminate, red arrows showing interfacial delamination events, (b) TOCNF + PVA – Epoxy A laminate, arrows showing intralayer damage within the layers.

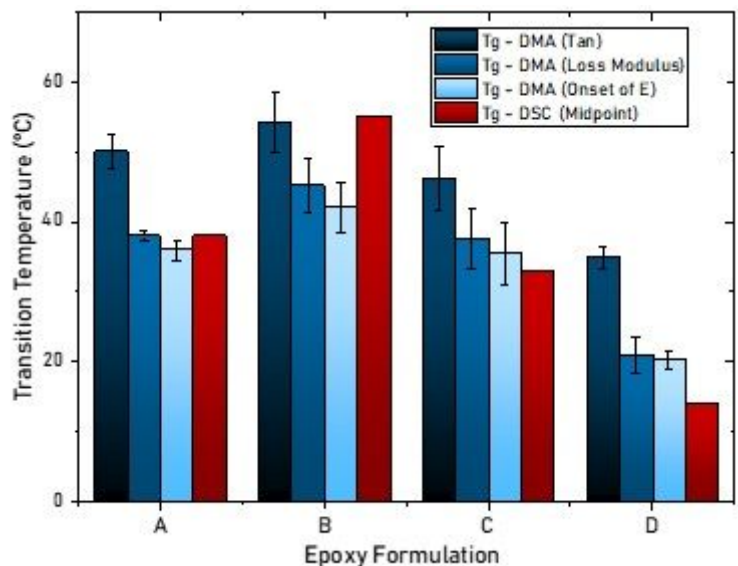


Figure 4

Glass transition temperature of different epoxy formulations as taken from DMA and DSC.

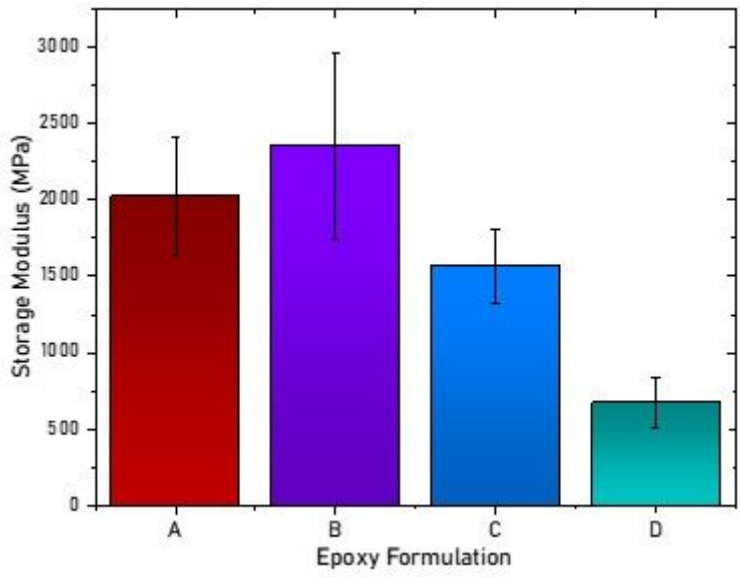


Figure 5

Storage modulus of different epoxy formulations as taken from the DMA.

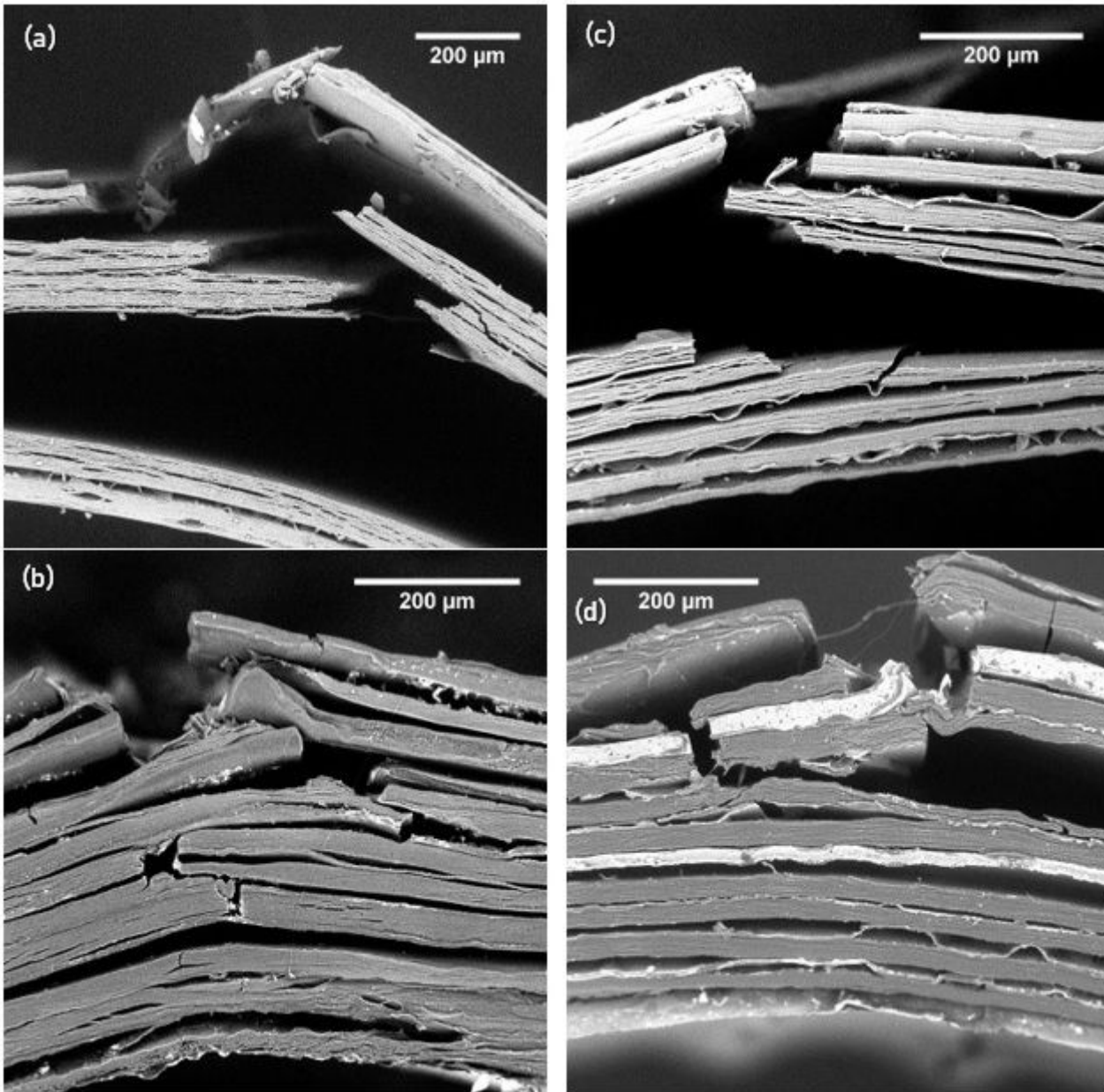


Figure 6

SEM images of the fracture behavior of 10 layer TOCNF film laminates with different epoxy formulations as interlayers. Images are presented in order of stiffness $a > b > c > d$. (a) TOCNF + PVA – Epoxy B (b) TOCNF + PVA – Epoxy A. (c) TOCNF + PVA – Epoxy C. (d) TOCNF + PVA – Epoxy D.

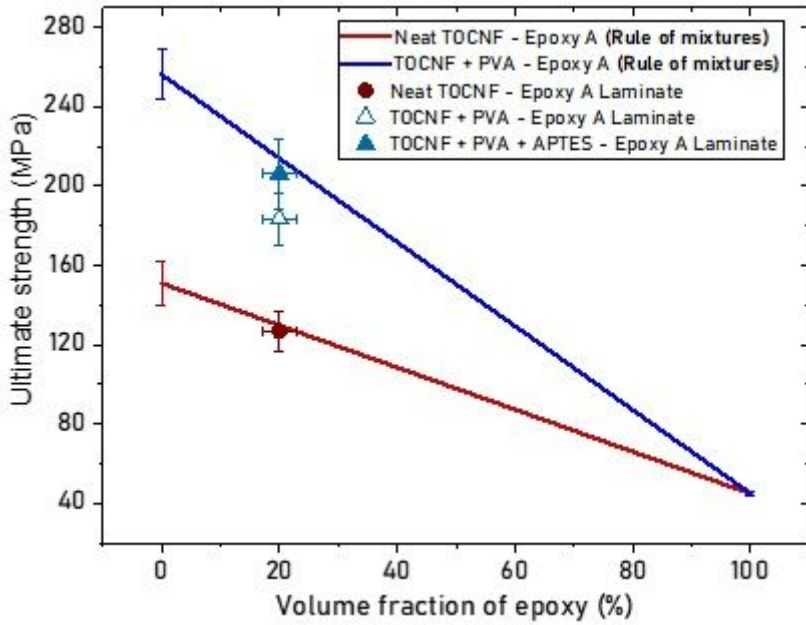


Figure 7

Tensile testing of different laminates. Blue and red lines represent the iso strain rule of mixtures of TOCNF + PVA – Epoxy A and Neat TOCNF – Epoxy A laminates.

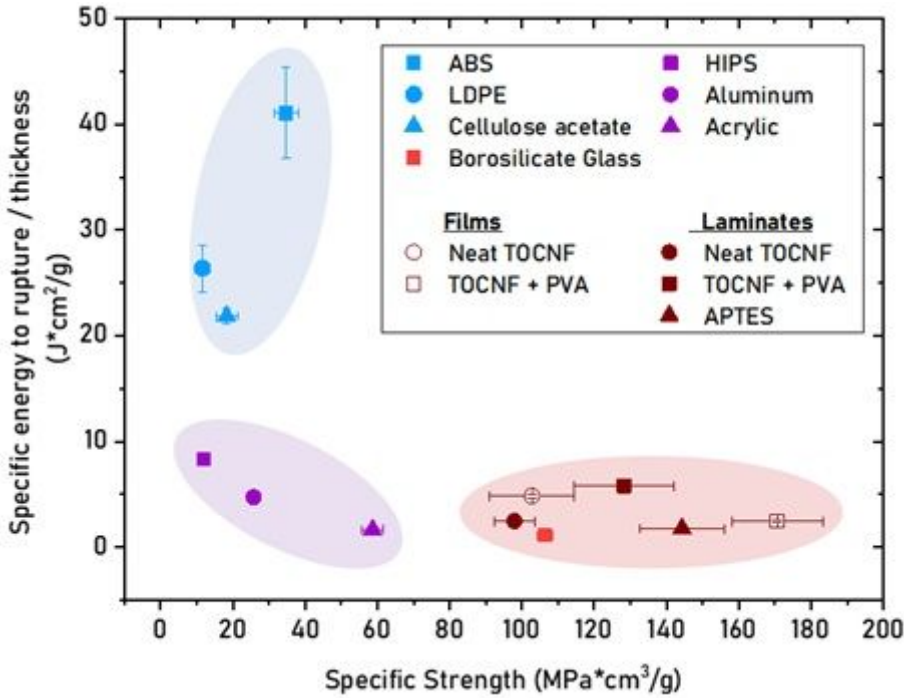


Figure 8

Plot shows specific energy to rupture divided by thickness (t) against the specific strength of various materials, including ABS, LDPE, Cellulose acetate, Acrylic, PS, Aluminum, Borosilicate Glass, Neat TOCNF and TOCNF + PVA films and 3 different 10 layers TOCNF or TOCNF + PVA laminates. Blue bubble are ductile polymers (low specific strength but high specific energy to rupture), purple bubble somewhat

brittle materials (low specific strength and energy to rupture), red bubble indicates high specific strength but low specific energy to rupture.

Supplementary Files

This is a list of supplementary files associated with this preprint. Click to download.

- [GraphicalAbstract.jpg](#)
- [SUPPORTINGINFORMATIONEnhancedTOCNFLaminates.docx](#)